3rd International Conference on Experiments/Process/System Modeling/Simulation & Optimization
3rd IC-EpsMsO
Athens, 8-11 July, 2009

A NOVEL MECHANISM TO PRODUCE FIGURE-EIGHT-SHAPED CLOSED CURVES IN THE THREE-DIMENSIONAL SPACE

Christopher G. Provatidis*

*Division of Mechanical Design and Control Systems, School of Mechanical Engineering
National Technical University of Athens, Greece
9 Heroes of Polytechnion Ave, GR-15780, Athens, Greece, tel: +30 210 772 1520, fax: +30 210 772 2347
Email: cprovat@central.ntua.gr, web page: http://users.ntua.gr/cprovat

Keywords: Mechanisms, propulsion, centrifugal force, antigravity, rotating mass.

Abstract. *This paper presents the concept of a novel mechanism that achieves to produce a special closed ∞-shaped curve in the three-dimensional space, along which two or more concentrated masses continuously move. In more details, the aforementioned path lies along the boundary (surface) of a sphere, thus possessing some remarkable properties. In addition, other curve configurations produced by different relationships between the angular velocities of the rolling components are discussed and relevant numerical results of the simulation are presented. In general, the findings of this work depict that this concept could inspire future applications.*

1 INTRODUCTION

An adequately detailed survey of antigravity and propulsive systems has been previously reported [1]. Concerning mechanical antigravity systems to which this paper belongs, the first relevant patent is probably due to Dean [2] (http://en.wikipedia.org/wiki/Dean_drive). An extension of this idea was made by Cook [3] who proposed a device that uses a couple of contra-rotating masses around a common axis, which transfers a mass from one rod to other, drawing an angle of 180 degrees. Later, Robertson [4] as well as Hoshino [5] proposed alternative ways to introduce eccentric masses of variable radius, aiming at reducing the centrifugal forces along the lower part of the mass track. Also, Chung [6] proposed a propulsion system based on the Coriolis force. Although electro-gravitics [7] and ion thrusters [8] is the tendency in non-conventional antigravity propulsion, within the years 1996-2002 NASA spent six whole years of research without a remarkable success [9,10]; an Internet search also reveals that some aerospace industries have simultaneously conducted a similar research.

Instead of using two synchronized and contra-rotating masses over a permanent vertical plane as in the case of the original Dean's drive, this paper investigates an alternative configuration in which the rotating masses move along a closed ∞-shaped curve within the three-dimensional space, in such a way that the reference vector $\vec{r}$ lies always in the half space below or beyond the centre of this curve (it draws an angle of 180 degrees). Initial results [11] and a detailed description [12,13] have been previously presented elsewhere.

2 DESCRIPTION OF MECHANISM

Between several alternative designs, this preliminary study concerns the primitive mechanism shown in Figure 1. The mechanism consists of a conventional planetary system (spin gears S1 and S2, planet gears P1 and P2), in which concentrated masses, i.e. mass (a) and mass (b), are attached perpendicularly to the shafts of the spin gears S1 and S2, respectively. Briefly, a motor drives the planet gear (P1) thus offering power transmission through P1-S1 towards the mass (a). Similarly, the rest half of the power produced by the motor is transmitted through P1-S2 towards the other mass (b).

A characteristic of this mechanism is that the second planet gear, P2, is fixed thus causing rolling of the spin gears S1 and S2 on P2. Obviously, the rotation of the planet gear P1 enforces the spin gear S1 to rotate about its local axis (initially coinciding with the global *z*-axis) and also enforces the casing to rotate around *x*-axis. When assuming the *same* diameters of the four gears (P1, P2, S1 and S2), due to the aforementioned rolling at the interface between P2 and S1:

- the spin gear S1 has an angular velocity ω that is half that of the motor ($\omega = \omega_{motor}/2$)
- the spin gear S2 has the *same* angular velocity but of opposite sign, $-\omega$
- the casing rotates with the same angular velocity, ω.

Regarding the sign of the angles, the convention is that positive angles are considered those formatted as (Ox,Oy), (Oy,Oz) and (Oz,Ox).

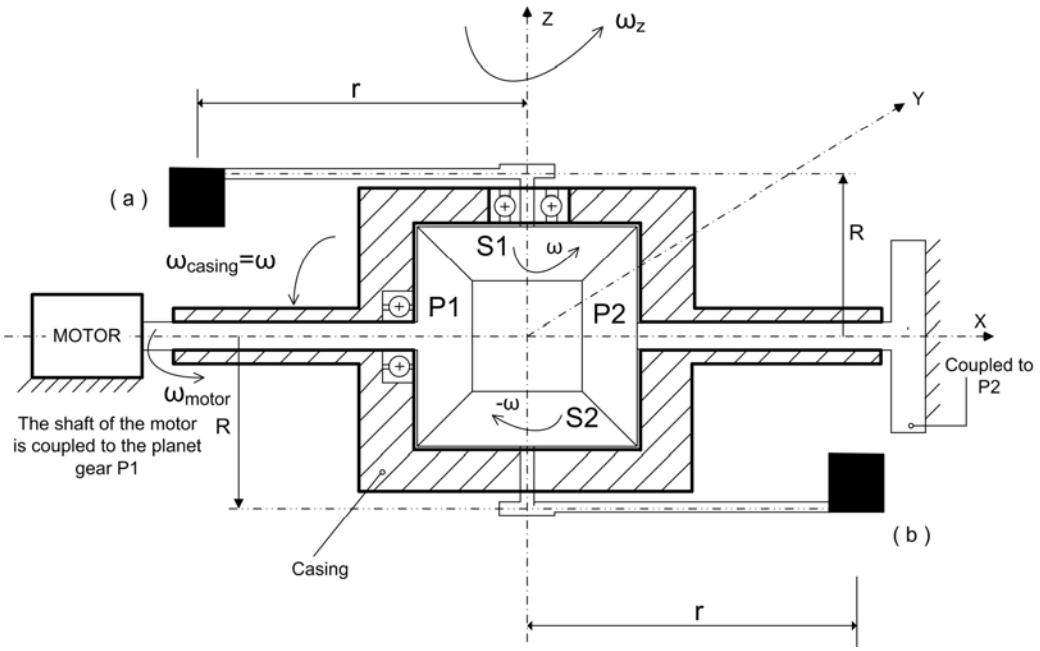

Figure 1: Abstractive sketch of the mechanism at the initial time instant ($t = 0$)

The characteristic dimensions of the mechanism are (Figure 1):

- the radius r of the level where the masses are attached and
- the radius R of the casing; more accurately it should be the distance between the *centroids* of the masses at the positions (a) and (b)

As shown in Figure 1, the initial coordinates of the masses, at time $t = 0$, are:

- Mass (a): $(x, y, z) = (-r, 0, +R)$, and Mass (b): $(x, y, z) = (+r, 0, -R)$

3 EQUATIONS OF MOTION

The description of section 2 reveals that each spin gear, S1 and S2, undertakes two simultaneous rotations, both of the same angular velocity, ω. In the general case, the first motion (rotation of S1) is related to an angle $\theta_1 = \omega_1 t$ about the z-axis, and corresponds to a relative rotation of the initial coordinate system by $\theta_1' = -\omega_1 t$, while the second motion (rotation of the casing about the x-axis by $\theta_2 = \omega_2 t$) is related to an relative angle $\theta_2' = -\omega_2 t$. Therefore, with respect to the global inertial Cartesian co-ordinate system Oxyz, the path followed by the rotating mass (a) is finally given by:

$$\begin{Bmatrix} x_a \\ y_a \\ z_a \end{Bmatrix} = \begin{bmatrix} 1 & 0 & 0 \\ 0 & \cos\omega_2 t & -\sin\omega_2 t \\ 0 & +\sin\omega_2 t & \cos\omega_2 t \end{bmatrix} \begin{bmatrix} \cos\omega_1 t & -\sin\omega_1 t & 0 \\ +\sin\omega_1 t & \cos\omega_1 t & 0 \\ 0 & 0 & 1 \end{bmatrix} \begin{Bmatrix} -r \\ 0 \\ +R \end{Bmatrix} = \begin{Bmatrix} -r\cos\omega_1 t \\ -r\sin\omega_1 t\cos\omega_2 t - R\sin\omega_2 t \\ -r\sin\omega_1 t\sin\omega_2 t + R\cos\omega_2 t \end{Bmatrix} \quad (1a)$$

Henceforth, we consider the particular case that: $\omega_1 = \omega_2 = \omega$, and therefore Eq(1) becomes:

$$x_a(t) = -r\cos\omega t,\ y_a(t) = -\left(r\sin\omega t\cos\omega t + R\sin\omega t\right),\ z_a(t) = -r\sin^2\omega t + R\cos\omega t \quad (1b)$$

Furthermore, the corresponding velocities are given as:

$$\dot{x}_a(t) = \omega r\sin\omega_1 t,\ \dot{y}_a(t) = -\left(\omega r\cos 2\omega t + \omega R\cos\omega t\right),\ \dot{z}_a(t) = -\left(r\omega\sin 2\omega t + \omega R\sin s\omega t\right), \quad (2)$$

while the corresponding accelerations are given as:

$$\ddot{x}_a(t) = \omega^2 r\cos\omega t,\ \ddot{y}_a(t) = 2\omega^2 r\sin 2\omega t + \omega^2 R\sin 2t,\ \ddot{z}_a(t) = -\left(2\omega^2 r\cos 2\omega t + \omega^2 R\cos\omega t\right) \quad (3)$$

In a similar way, the path of the mass (b), as well as the velocity and accelerations components, is given by:

$$x_b(t) = r\cos\omega t,\ y_b(t) = -r\sin\omega t\cos\omega t + R\sin\omega t,\ z_b(t) = -\left(r\sin^2\omega t + R\cos\omega t\right) \quad (4)$$

Also:

$$\dot{x}_b(t) = -\omega^2 r\cos\omega t,\ \dot{y}_b(t) = -\omega r\cos 2\omega t + \omega R\cos\omega t,\ \dot{z}_b(t) = -\omega r\sin 2\omega t + \omega R\sin\omega t \quad (5)$$

and also:

$$\ddot{x}_b(t) = -\omega^2 r\cos\omega t,\ \ddot{y}_b(t) = 2\omega^2 r\sin 2\omega t - \omega^2 R\sin\omega t,\ \ddot{z}_b(t) = -\left(2\omega^2 r\cos 2\omega t - \omega^2 R\cos\omega t\right) \quad (6)$$

4 GEOMETRIC PROPERTIES OF THE PATH

Concerning the properties of the path on which the masses (a) and (b) move, using Eq(1) and Eq(4), it can be proven that:

1) Both masses move on the *same* path, and each of them gives away to the other. For example, when the spin gear S1 rotates by 90 degrees ($\omega t = \pi/2$), the co-ordinates of the mass (a) become (x, y, z) = (+r, 0, -R), which means that it takes the initial position of (b) shown in Figure 1. In a similar way, the co-ordinates of the mass (b) become (x, y, z) = (-r, 0, +R), which means that it takes the initial position of (a) shown in Figure 1. The same happens after 90 degrees of further rotation of the casing around x-axis (and simultaneous rotation of S1 and S2 by also 90 degrees), and so on.

2) All points of the abovementioned path belong to a sphere of radius, i.e.:

$$x_a^2 + y_a^2 + z_a^2 = x_b^2 + y_b^2 + z_b^2 = r_{sphere}^2 \text{, with } r_{sphere} = \sqrt{r^2 + R^2} \tag{7}$$

3) The point, I, at which the patch intersects itself, is found at the place (see *Appendix*):

$$x_{\text{intersect}} = +R, \;\; y_{\text{intersect}} = 0, \;\; z_{\text{intersect}} = -r \tag{8}$$

As a consequence of eq(8), it is worth-mentioning that in the hypothetical case that $R = 0$, the intersection I lies along the z-axis ($x_{\text{intersect}} = 0, \;\; y_{\text{intersect}} = 0$).

4) The co-ordinates of the centroid of the couple (a,b) are:

$$\begin{aligned} x_{cm}(t) &= \frac{1}{2}\left[x_a(t) + x_b(t)\right] \equiv 0 \\ y_{cm}(t) &= \frac{1}{2}\left[y_a(t) + y_b(t)\right] = -r\sin\omega t\cos\omega t = -\frac{1}{2}r\sin 2\omega t \\ z_{cm}(t) &= \frac{1}{2}\left[z_a(t) + z_b(t)\right] = -r\sin^2\omega t \end{aligned} \tag{9}$$

Obviously, since it holds that:

$$x_{cm}^2(t) + y_{cm}^2(t) + \left[z_{cm}(t) + r/2\right]^2 = (r/2)^2, \tag{10}$$

it is evident that the centroid of the two masses moves on the yz-plane along the circumference of a circle of radius $(r/2)$, centered at the point $(0, 0, -r/2)$.

5 INDUCED INERTIAL FORCES

Using Eq(1)-Eq(6) in combination with Newton's Second Law [2], the inertial force components at each makeweight are given by:

$$\begin{aligned} F_{a,x} &= -m\ddot{x}_a(t) = -m\omega^2 r\cos\omega t \\ F_{a,y} &= -m\ddot{y}_a(t) = -m\left(2\omega^2 r\sin 2\omega t + \omega^2 R\sin 2t\right) \\ F_{a,z} &= -m\ddot{z}_a(t) = +m\left(2\omega^2 r\cos 2\omega t + \omega^2 R\cos\omega t\right) \end{aligned} \tag{11}$$

and

$$\begin{aligned} F_{b,x} &= -m\ddot{x}_b(t) = +m\omega^2 r\cos\omega t \\ F_{b,y} &= -m\ddot{y}_b(t) = -m\left(2\omega^2 r\sin 2\omega t - \omega^2 R\sin\omega t\right) \\ F_{b,z} &= -m\ddot{z}_b(t) = +m\left(2\omega^2 r\cos 2\omega t - \omega^2 R\cos\omega t\right) \end{aligned} \tag{12}$$

Therefore, the resultant inertial force components in the entire mechanism are given by:

$$\begin{aligned} F_x &= F_{a,x} + F_{b,x} \equiv 0 \\ F_y &= F_{a,y} + F_{b,y} = -4m\omega^2 r\sin 2\omega t \\ F_z &= F_{a,z} + F_{b,z} = +4m\omega^2 r\cos 2\omega t \end{aligned} \tag{13}$$

We notice that while in the x-direction there is no resultant force, in contrast, harmonic components exist in the y- and z-directions. Most interesting, the vertical z-component is of amplitude $4m\omega^2 r$ and appears a maximum upward value at $\omega t = 0, \pi, 2\pi, 3\pi, \ldots$, while it appears the *same* downward value at $\omega t = \pi/2, 3\pi/2, 5\pi/2, \ldots$

6 MOMENTS AND POWER

With respect to the *x*-axis the induced moments of the inertial forces at the makeweights are found as:

$$M_x = M_{a,x} + M_{b,x} = -2m\omega^2 r^2 \sin 2\omega t \tag{14}$$

Also, the power spent by the electric motor is calculated using the classical consideration of the inertial forces through the formula

$$P = -m\left(\ddot{x}_a\dot{x}_a + \ddot{y}_a\dot{y}_a + \ddot{z}_a\dot{z}_a + \ddot{x}_b\dot{x}_b + \ddot{y}_b\dot{y}_b + \ddot{z}_b\dot{z}_b\right) \tag{15}$$

which, in virtue of Eqs(1-6), leads to:

$$P(t) = -m\omega^3 r^2 \sin 2\omega t \tag{16}$$

7 KINETIC AND POTENTIAL ENERGY

Kinetic, $E_{kinetic}$, and potential, $E_{potential}$, energy of the couple of masses (a) and (b) is given by:

$$\begin{aligned} E_{kinetic} &= \frac{1}{2}m\left[\left(\dot{x}_a^2 + \dot{y}_a^2 + \dot{z}_a^2\right) + \left(\dot{x}_b^2 + \dot{y}_b^2 + \dot{z}_b^2\right)\right] = \\ &= m\omega^2\left[R^2 + r^2\left(1 + \sin^2\omega t\right)\right] \end{aligned} \tag{17}$$

and

$$E_{potential} = -2mgr\sin^2\omega t \tag{18}$$

8 WORK OF INERTIAL FORCES

Integrating Eq(16), the work spent from $t = 0$ until to every other time t is given by:

$$W(t) = -\int_0^t P(\tau)\,d\tau = 2m\omega^2 r^2 \sin^2\omega t \tag{19}$$

One can easily validate that the work given by Eq(19) equals to the change of the kinetic energy, as always happens. The sign (-) in Eq(19) was put in order to depict that the real resultant is $m_a\ddot{\vec{r}}$, while the inertial force was taken as $-m_a\ddot{\vec{r}}$.

9 APPLICATIONS

9.1 Typical paths

For time instances so that $0 \le \omega t \le \pi/2$, a typical path followed by the masses (a) and (b) is illustrated in Figure 2. One can notice that the path is a continuous ∞-shaped curve of unequal loops. Clearly, when the casing and the spin gear rotate by 90 degrees, the mass (a) completes the blue line while the mass (b) completes the red line. For $\pi/2 \le \omega t \le \pi$, the mass (a) follows exactly the path already completed by the mass (b), while the mass (b) follows exactly the path already completed by the mass (a), and so on! In other words, the masses (a) and (b) *mutually offer space to each other*.

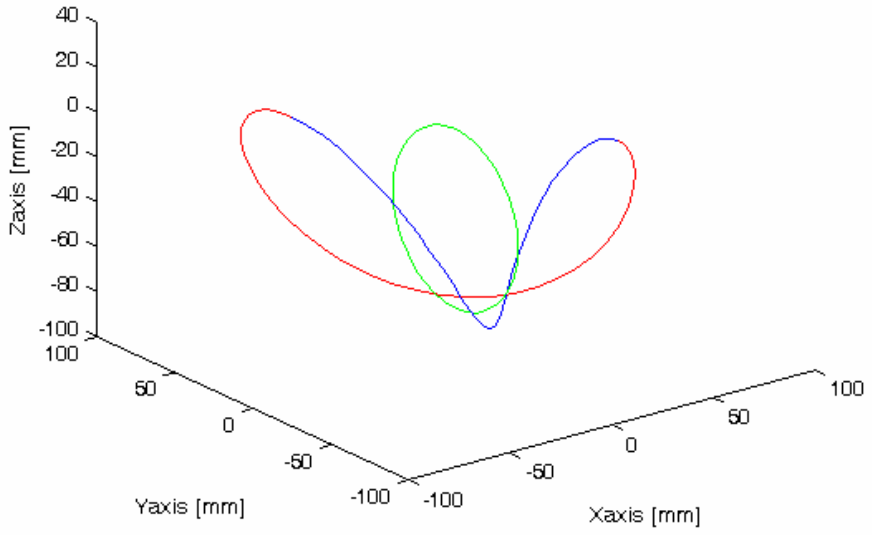

Figure 2: Patch of the masses and their centroid (r =80mm, R=25mm). The blue line corresponds to the mass (a), the red one to the mass (b), while the green corresponds to the centroid.

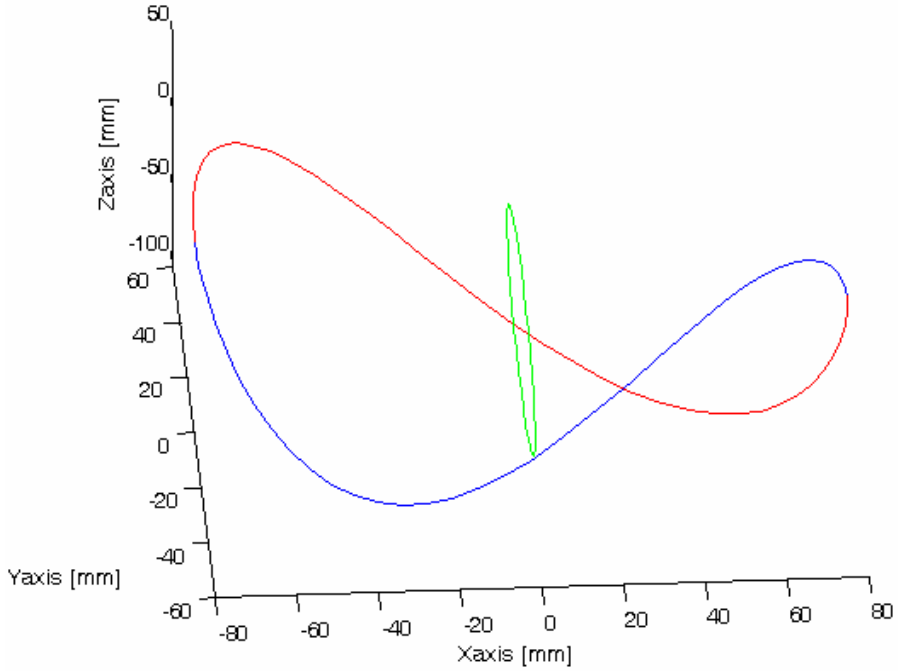

Figure 3: A different perspective view for the conditions of Figure 2.

In order to have a better feeling of the path, its *asymmetry* and its unique *intersection* point I, as well as the circle followed by the centroid of the two rotating masses (a) and (b), are all shown in Figure 3.

9.2 Simulation of forces and power

The resultant of the vertical force components are shown in Figure 4, where the *x*-, *y*- and *z*-components are illustrated in blue, red and green colour, respectively. The *z*- force component (F_z), which is in green colour, is of major importance as it is related to the ability of the mechanism to move upwards. One can notice in Figure 4 an alternating time history, thus causing no upward impulse.

In more details, when the masses are found exactly as in Figure 4 (at initial time: $t = 0$, Angle = 0 degrees), the resultant vertical force is *positive* (upwards) and it is very similar for both masses (identical only when $R = 0$), while the ***same*** value but of *negative* sign appears at the angle of 90 degrees.

Moreover, concerning the power transmitted generated by the motor and then transmitted to the masses is shown in Figure 5, in which the friction has been neglected. The maximum power appears at $\theta_1 = \pi/4$.

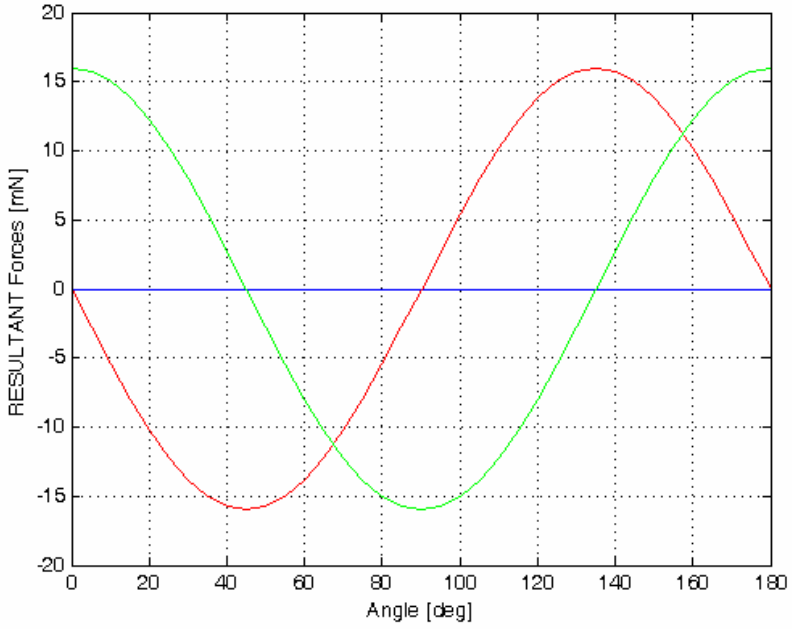

Figure 4: Centrifugal force components (blue: Fx, red: Fy, green: Fz). Data: (r =80mm, R=25mm).

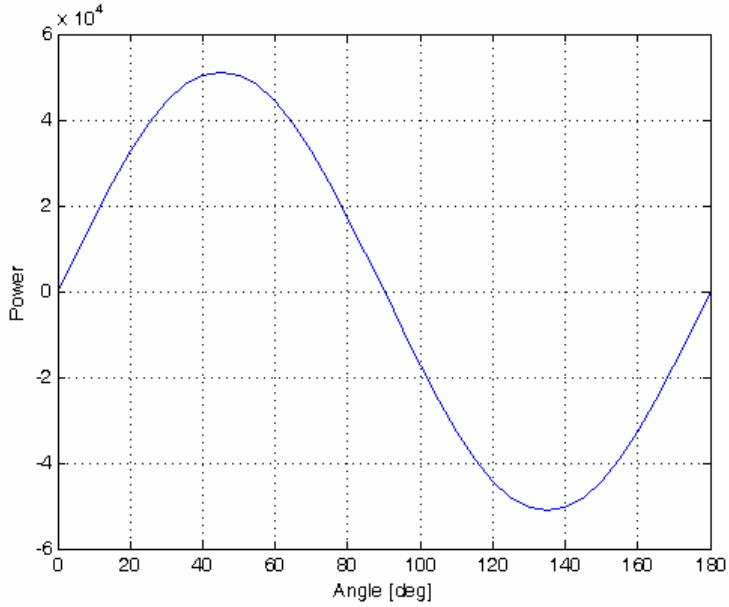

Figure 5: Time history of the motor power (r =80mm, R=25mm).

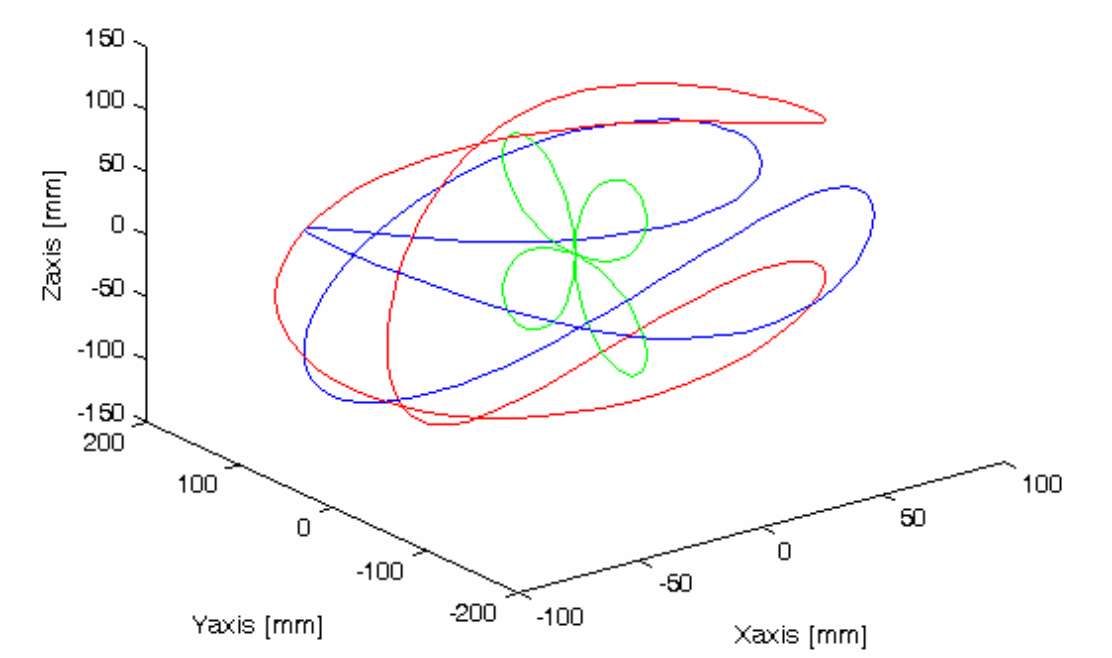

Figure 6: Paths of the masses. The blue line corresponds to the mass (a), the red to the mass (b) while the green to their centroid. (r =100mm, R=60mm, $\omega_{casing}=\omega_{spin\ gear}/2$)

9.3 Modification of the mechanism

Using a different configuration, it could be possible to modify the angular velocity of the casing, so that it obtains, for example, half the value of the spin gear S1 ($\omega_{casing}=\omega_{spin\ gear}/2$). In such as case, the corresponding paths of the two masses *do not coincide* but they are quite distinct as shown in Figure 6. In more details, the masses (a) and (b) follow the blue and red lines, respectively, while their centroid forms an exotic shape of a *tetrafilon* (four-leaf) flower!

It is also worth-mentioning that in the abovementioned case, not one (I) but two intersections of the path appear.

A more close investigation reveals that the motion sequence of the centroid along the tetrafilon is according to the sequence (1→2→3→4→5→6→7→8→9≡1) shown in Figure 7.

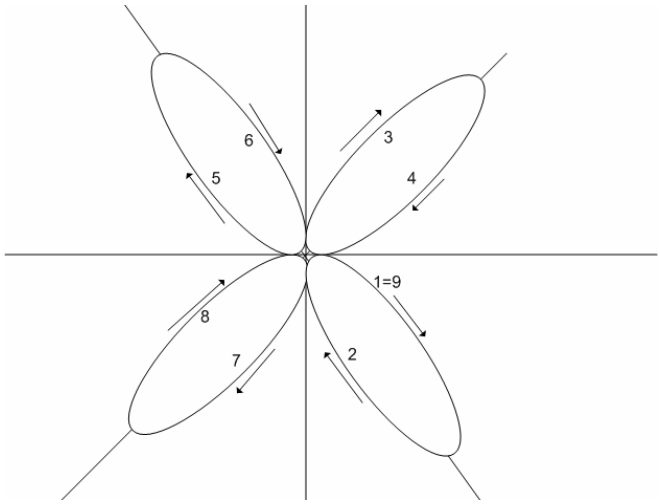

Figure 7: Motion sequence of the centroid along the tetrafilon (shown in Figure 6)

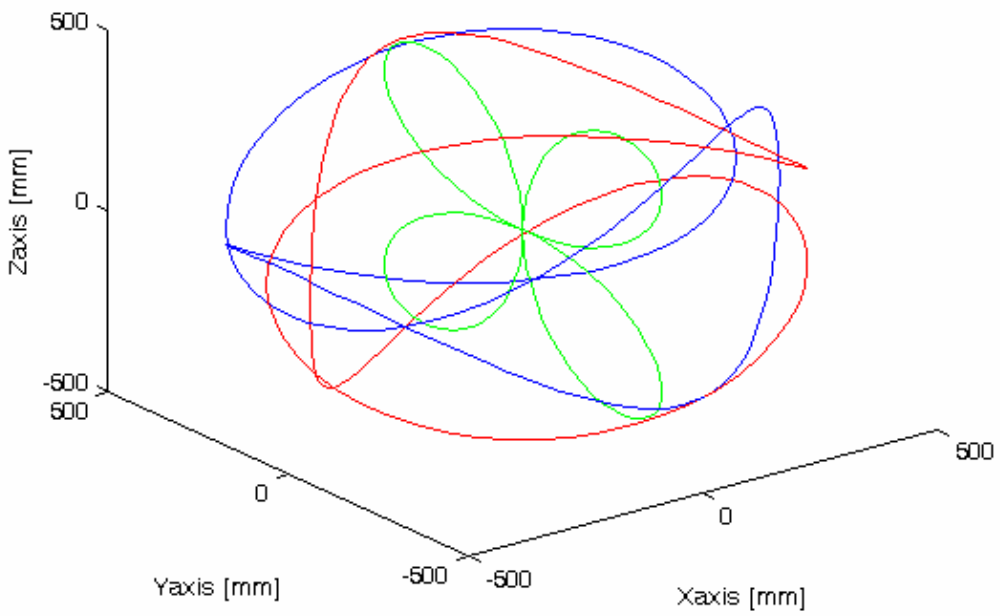

Figure 8: Paths of the makeweights and their centroid (r = 500mm, R = 60mm).

Remark: Preserving the diameter of the casing and increasing the radius of the concentrated mass, for example, choosing r = 500mm, R = 60mm, the paths become as those shown in Figure 8. In other words, the longer the radius r becomes the larger the extreme loops become, by also increase of the four-leaf shape.

10 DISCUSSION AND CONCLUSIONS

The principle of a novel mechanism has been presented in full detail. Not only its operation but also closed-form analytical expressions of kinematics and dynamics have been reported. Concerning its possibility to obtain a propulsion, when applying the second Newton's law towards the vertical direction, similar equations with those obtained in Ref[1] were received, a fact that dictates that an upwards motion is again possible. This happens under the condition that a considerable angular velocity has been obtained, before the object to which the proposed mechanism has been attached is left free to move. The only difference is that instead of leaving the object free when the rigid bars are at the horizontal position moving upwards as happened in Ref[1], in the present case the maximum altitude is achieved when these bars are found at the position $\phi = -\pi/4$ thus leaving sufficient path at which the centrifugal forces are positive.

In this preliminary report the case of a rotation around the vertical axis ($\omega_z \neq 0$) has been omitted, but a detailed report is in preparation.

Acknowledgements

I acknowledge Mr. Theodore Tsiriggakis for our close cooperation on patent applications since 1982, as well as his son Vassilis Tsiriggakis for our cooperation during the last three years where this project was finalized.

References

[1] Provatidis, C.G. (2009), "Some issues on mechanical antigravity mechanisms using two contra-rotating masses", Proceedings 3rd IC-EpsMsO, Athens, 8-11 July, 2009
[2] Dean, N.L. (1959) "System for converting rotary motion into unidirectional motion", US Patent 2,886,976 (Filed Jul. 13, 1954, granted May 19, 1959). See, also: http://www.rexresearch.com/dean/dean.htm
[3] Cook, R.L. (1980) "Device for Conversion of Centrifugal Force to Linear Force and Motion", US Patent 4,238,968, Dec. 16, 1980.
[4] Robertson, D.B. (2001) "Propulsion method and apparatus utilizing centrifugal force", World Intellectual Property Organization (WIPO), International Publication Number WO 01/46584 A3, 28 June 2001.
[5] Hoshino M. (2005) "Propulsion apparatus using centrifugal force", US Patent 20050139022 (Filing data: Jan. 7, 2004, Publication date: June 30, 2005)
[6] Chung T.B. (2003) "Internal propulsion apparatus of closed system using a Coriolis force", International Patent WO 03/087574 A1, 23 (International filing date: 08 April 2003; Publication date: 23 October 2003)
[7] LaViolette, P.A. (2008) "Secrets of Antigravity Propulsion: Tesla, UFOs, and Classified Aerospace Technology", Bear & Company, Rochester, Vermont (ISBN: 978-1-59143-078-0)
[8] Goebel, D.M., Katz, I. (2008) "Fundamentals of Electric Propulsion: Ion and Hall Thrusters", Wiley.
[9] Millis, M.G., Thomas, N.E. (2006), "Responding to Mechanical Antigravity, NASA/TM-2006-214390, AIAA-2006-4913, December 2006. Available at: http://gltrs.grc.nasa.gov/reports/2006/TM-2006-214390.pdf
[10] Millis, M.G. (2005), "Assessing Potential Propulsion Breakthroughs". In New Trends in Astrodynamics and Applications. ed. Edward Belbruno. New York: Annals of the New York Academy of Sciences (1065), 441–461 (doi: 10.1196/annals.1370.023).
[11] Provatidis, C. (2008) "Analytical model of a promising novel mechanism", Internal Report MD&CS-888, National Technical University of Athens, Mechanical Engineering Department, August 2008. Available in: http://users.ntua.gr/cprovat/yliko/English_Tsiriggakis_Model_Motor1.pdf, since August 2008.
[12] Tsiriggakis, V. et al. (2008), "Antigravity Mechanism", US Patent Application No.61/110,307 (Filing date: Oct. 31, 2008).
[13] Tsiriggakis, Th. (2009)"The Greek Antigravity Mechanism", TRITO MATI (http://www.tritomati.gr), Vol.167 (January), pp. 26-30.

APPENDIX: Intersection of the ∞-shaped path

In fact, if the rotating mass (a) is as shown in Figure 1 (at time $t = 0$), then at a later time t' that fulfills the relationship:

$$\cos\omega t' = -R/r\,, \tag{20}$$

The corresponding coordinates of the rotating mass (a) will be given by:

$$\begin{aligned} x_a(t') &= -r\cos\omega t' = -r\left(-R/r\right) \equiv +R \\ y_a(t') &= -\sin\omega t'\left(r\cos\omega t' + R\right) \equiv 0 \\ z_a(t') &= -r\sin^2\omega t' + R\cos\omega t' = -r\left(1-\cos^2\omega t'\right) + R\cos\omega t' \\ &= -r\left(1-R^2/r^2\right) + R\left(-R/r\right) = -r + \left(R^2/r - R^2/r\right) \equiv -r \end{aligned} \tag{21}$$

In the sequence, we shall prove that through the same point, I, the rotating mass (b) has earlier passed. In fact, if we choose the time t'', such as:

$$\cos\omega t'' = +R/r\,, \tag{22}$$

The coordinates of the mass (b) are given by:

$$\begin{aligned} x_b(t'') &= +r\cos\omega t'' = +r\left(+R/r\right) \equiv +R \\ y_b(t'') &= -r\sin\omega t''\cos\omega t'' + R\sin\omega t'' = \sin\omega t''\left(-r\cos\omega t'' + R\right) \\ &= \sin\omega t''\left[-r\left(+R/r\right) + R\right] \equiv 0 \\ z_b(t'') &= -\left(r\sin^2\omega t'' + R\cos\omega t''\right) = -\left[r\left(1-\cos^2\omega t'' + R\cos\omega t''\right)\right] \\ &= -\left[r\left(1-\cos^2\omega t'' + R\cos\omega t''\right)\right] = -\left[r\left(1-\left(+R/r\right)^2 + R\left(+R/r\right)\right)\right] \\ &= -\left[r - r\left(+R^2/r^2\right) + \left(+R^2/r\right)\right] = -\left[r - \left(R^2/r\right) + \left(R^2/r\right)\right] \equiv -r \end{aligned} \tag{23}$$

Equation (23) proves that the time instants t' and t'' correspond to the intersection I of the path, which the masses (a) and (b), respectively, pass through. Obviously, it holds that $t'' < t'$, and also, $\theta_1(t') > \pi/2$, $\theta_1(t'') < \pi/2$, $\theta_1(t') = \pi - \theta_1(t'')$.